



Journal homepage: <http://civiljournal.semnan.ac.ir/>

Damage Detection of Bridge by Rayleigh-Ritz Method

M.H. Daneshvar¹, A.R. Gharighoran^{2*}, S.A. Zareei³ and A.Karamodin⁴

1. Ph.D. Candidate, Department of Civil Engineering, Isfahan (Khorasgan) Branch, Islamic Azad University, Isfahan, Iran

2. Associate Professor, Faculty of Civil Engineering and Transportation, University of Isfahan, Isfahan, Iran

3. Associate Professor, Department of Civil Engineering, Isfahan (Khorasgan) Branch, Islamic Azad University, Isfahan, Iran

4. Associate Professor, Department of Civil Engineering, Ferdowsi University, Mashhad, Iran

Corresponding author: a.gharighoran@trn.ui.ac.ir

ARTICLE INFO

Article history:

Received: 15 April 2019

Accepted: 10 October 2019

Keywords:

Damage Detection,
Rayleigh-Ritz,
Mode Shapes,
Natural Frequency.

ABSTRACT

As a result of environmental and accidental actions, damage occurs in structures. The early detection of any defect can be achieved by regular inspection and condition assessment. In this way, the safety and reliability of structures can be increased. This paper is devoted to proposing a new and effective method for detecting, locating, and quantifying beam-like structures. This method is based on the Rayleigh-Ritz approach and requires a few numbers of natural frequencies and mode shapes associated with the undamaged and damaged states of the structure. The great advantage of the proposed approach against the other methods is that it considers all kinds of boundary and damping effects. To detect damage using the penalty method, this article considers lumped rotational and translational springs for determining the boundary conditions. The results indicate that the proposed method is an effective and reliable tool for damage detection, localization, and quantification in the beam-like structures with different boundary conditions even when the modal data are contaminated by noise.

1. Introduction

In civil, mechanical, and aerospace engineering, damage diagnosis of structures has received considerable attention from researchers. Damage detection methods provide the continuous inspection of the

safety and integrity of structures. Four main levels of these techniques are detection, localization, severity investigation, and also structure remained life estimation [1]. Up to now, a large amount of damage detection strategies have been developed. Most of them are based on the finite element method

(FEM) [1, 2]. It is worth emphasizing that the structural responses and modal parameters are the functions of the mechanical properties of the structure. Hence, any changes in the physical characteristics of a structure will alter the responses. Accordingly, the damage diagnosis schemes based on FEM have been established. These techniques update the FEM model to match the analytical and measured data. In this way, the mechanical parameters of the damaged structure can be estimated. These techniques are divided into two groups, including the static and dynamic approaches. In the latter one, the modal parameters such as the natural frequencies and mode shapes are used, and the responses such as displacements and strains are measured in static approaches [3, 4]. It should be mentioned that some of the damage identification techniques take advantage of both static and dynamic data. In the following, the well-known damage detection methods of beams are reviewed briefly.

In 1996, Stubbs and Kim [5] found the damage location without using the baseline modal parameter in a two-span concrete beam by utilizing FEM. With the help of dynamic stiffness, Maeck *et al.* [6] proposed two strategies for detecting stiffness degradation in reinforced concrete beams. They validated their method by performing experiments. In another research work, Maeck and De Roeck [7] assessed gradually damaged reinforced concrete beams by calculating the modal bending moments and curvatures. Moreover, Kokot and Zembaty [8] measured both translational and rotational degrees of freedom for damage detection of beams. In this research, a minimization

problem was solved. By using the global fitting technique, Myung-Keun *et al.* [9] located damage in beams. Note that this algorithm was the extension of the gapped fitting method. By employing time modal features and artificial neural networks, Park *et al.* [10] presented a sequential damage detection method for beams. Their approach included two phases consisting of time-domain and modal-domain damage monitoring. Sung *et al.* [11] deployed modal flexibility for damage detection of cantilever beam-type structures. Additionally, Eraky [12] used a damage index algorithm as a tool for localizing damages that occurred in flexural structural elements. This index was based on modal strain energy. Then, they experimentally verified the mentioned algorithm. Limongelli [13] carried out experiments on a post-tensioned concrete beam for assessing the possibility to detect early warning signs of deterioration based on static and/or dynamic tests. In most of the damage detection methods, FEM was employed. Although the FEM scheme has extensively been utilized in damage detection of structures, only a few approaches are developed based on the well-known Rayleigh-Ritz technique. These strategies are briefly reviewed below.

Deobald and Gibson [14] utilized the Rayleigh-Ritz algorithm for finding the elastic constants of the orthotropic plates with clamped and free edges. Cao and Zimmerman [15] deployed the Ritz vector to monitor the health of structures. In this process, the minimum rank perturbation theory was utilized. Also, these researchers concluded that the Ritz vectors are more sensitive to damage than the mode shapes.

Based on the Rayleigh-Ritz approach, Li *et al.* [16] specified the location of damage in plate-like structures. Moreover, they suggested two new damage indices based on modal strain energy. Afterward, Sohn and Law [17] applied load-dependent Ritz vectors in Bayesian probabilistic damage detection. In 2011, Sarker *et al.* [18] employed the Ritz method for damage detection of the circular cylindrical shell. García *et al.* [19] proposed a new technique for damage localization in laminated composite plates by using mode shape derivatives. Moreover, they suggested another damage detection approach for localizing the damage in the above-mentioned plates. In this approach, they took advantage of the higher-order derivatives, and in a similar manner, they utilized the Ritz technique. Maghsoodi *et al.* [20] presented a simple technique for detecting, locating, and quantifying multiple cracks in Euler–Bernoulli multi-stepped beams. To model cracks, they used rotational springs. They observed that the location and severity of damage were related to the natural frequencies of the beam. In this work, global interpolation functions were utilized the same as Rayleigh-Ritz method, instead of applying piecewise continuous mode shapes for a multi-step beam. Gharighoran [21] deployed the Ritz strategy for damage detection of reinforced and post-tensioned concrete beams. This technique was only applicable to simply supported beams.

This paper aims to propose a simple and robust method based on the Ritz scheme for locating and quantifying damage in beam-like structures with any kinds of boundary conditions. In fact, this work is an

improvement on the technique proposed by Gharighoran *et al.* [21]. In this study, the damage is modeled by reducing flexural stiffness. Moreover, the proposed strategy requires some of the natural frequencies and mode shapes of the healthy and damaged structure.

2. Governing Equations

Considering the natural frequencies and mode shapes, in general, the structural motion could not be harmonic. However, there are certain special initial displacements that will cause harmonic vibrations. These special initial deflections are called mode shapes, and the corresponding frequencies of vibration are called natural frequencies. Both of these parameters are related and could be captured by mass and stiffness matrices. The differential equation which governs the free vibration behavior of the beam has the subsequent equation [22]:

$$\mathbf{M}\ddot{\mathbf{Z}} + \mathbf{C}\dot{\mathbf{Z}} + \mathbf{K}\mathbf{Z} = \mathbf{0} \quad (1)$$

In which \mathbf{M} , \mathbf{C} , and \mathbf{K} denote mass, damping and stiffness matrices, respectively. Moreover, $\ddot{\mathbf{Z}}$, $\dot{\mathbf{Z}}$, and \mathbf{Z} are the acceleration, velocity, and displacement vectors, respectively. If the proportional damping is deployed, Eq. (1) can be rewritten as follows [22]:

$$\mathbf{M}\ddot{\mathbf{Z}} + \mathbf{K}_d\mathbf{Z} = \mathbf{0} \quad (2)$$

$$\mathbf{K}_d = \mathbf{K} + \mathbf{H}\mathbf{j}; \quad \mathbf{j} = \sqrt{-1} \quad (3)$$

Where \mathbf{H} denotes the Rayleigh's damping matrix, which can be expressed as [22]:

$$\mathbf{H} = \alpha\mathbf{K} + \beta\mathbf{M} \quad (4)$$

In this expression, α and β are constant values [22]. Accordingly, the following

equations can be achieved for the damped and un-damped structures, respectively[21]:

$$\mathbf{K}\Psi_p = \omega_p^2 \mathbf{M}\Psi_p \quad p=1, \dots, r \quad (5)$$

$$\mathbf{K}\bar{\Psi}_p = \bar{\omega}_p^2 \mathbf{M}\bar{\Psi}_p \quad p=1, \dots, r \quad (6)$$

where the p^{th} natural frequencies of the damped and un-damped structures are shown by $\bar{\omega}_p$ and ω_p , respectively. Furthermore, the p^{th} mode shapes of the damped and un-damped structures are $\bar{\Psi}_p$ and Ψ_p , respectively. Additionally, \mathbf{K}_d denotes the damped stiffness matrix. Besides, r is the number of mode shapes taken into account.

As a result of damage, the characteristics of matrices of the structure are altered. Consequently, Eqs. (5) and (6) change into the following forms [21]:

$$\hat{\mathbf{K}}\hat{\Psi}_p = \hat{\omega}_p^2 \hat{\mathbf{M}}\hat{\Psi}_p \quad p=1, \dots, s \quad (7)$$

$$\hat{\mathbf{K}}_d \hat{\Psi}_p = \bar{\omega}_p^2 \hat{\mathbf{M}}\hat{\Psi}_p \quad p=1, \dots, s \quad (8)$$

where the p^{th} natural frequencies of the damped and undamped damaged structures are shown by $\hat{\omega}_p$ and $\bar{\omega}_p$, respectively. Furthermore, the p^{th} mode shapes of the damped and undamped structures are $\hat{\Psi}_p$ and $\bar{\Psi}_p$, respectively. Additionally, $\hat{\mathbf{K}}_d$ and $\hat{\mathbf{K}}$ denote the damped and un-damped stiffness matrix of the damaged structure, respectively. Also, $\hat{\mathbf{M}}$ is the mass matrix of the damaged structure. Besides, p is the number of available mode shapes of the damaged structure. Accordingly, the subsequent orthogonality conditions can be obtained[21]:

$$\hat{\Psi}_p^T \hat{\mathbf{M}}\hat{\Psi}_q = \delta_{pq} \quad (9)$$

$$\hat{\Psi}_p^T \hat{\mathbf{K}}\hat{\Psi}_q = \hat{\omega}_q^2 \delta_{pq} \quad (10)$$

$$\hat{\Psi}_p^T \hat{\mathbf{K}}_d \hat{\Psi}_q = \bar{\omega}_q^2 \delta_{pq} \quad (11)$$

where δ is the Kronecker delta operator. In usual, it is assumed that the mass matrix of the damaged and undamaged structure are

similar [23]. As a consequence, only their stiffness matrices are different.

3. Damage Index

In this section, a local index is introduced for describing the damage. The global behavior of the structure is dependent on this parameter. In other words, it is sensitive to structural changes induced by the occurrence of damage. In finite element formulations, the damage is generally represented by a reduction in the stiffness of the individual finite elements, and it is presumed that the elemental stiffness matrix decreases uniformly due to damage. Therefore, damage identification is conducted at the element level. The change of the stiffness of the e^{th} element can be defined as follows [21]:

$$k_{Se} = k_e - \hat{k}_e \quad (11)$$

In this relation, k_e and \hat{k}_e are the stiffness matrices of the e^{th} element before and after the occurrence of damage, respectively. The stiffness matrix of the damaged element is given by [21]:

$$\hat{\mathbf{k}}_e = (1 - \alpha_{Se})\mathbf{k}_e \quad (12)$$

where α_{Se} denotes the sound index of the element. This parameter ranges from 0 to 1. If the e^{th} element is completely destroyed, α_{Se} is equal to 1. On the other hand, α_{Se} is zero when it is healthy. Accordingly, the damage index can be expressed as the following form:

$$\alpha_{De} = 1 - \alpha_{Se} \quad (13)$$

Therefore, the damage index of a beam element is written as [21]:

$$\alpha_{De} = \frac{(\hat{EI})_e}{(EI)_e} \quad (14)$$

In this equation, $(\hat{EI})_e$ and $(EI)_e$ are the flexural stiffness of the e^{th} element after and prior to damage, respectively. Accordingly,

the global stiffness matrix of a damaged structure can be expressed as [21]:

$$\hat{\mathbf{K}} = \sum_{e=1}^m \alpha_{De} \mathbf{K}_e \tag{15}$$

It should be mentioned that m is the number of elements.

4. Formulating the Damage Detection Problem Using the Ritz Method

The strain energy of the Euler-Bernoulli beam depicted in Fig. 1, can be computed as follows [24]:

$$\Pi = \frac{1}{2} \int_0^L EI(x) \left(\frac{d^2 w(x)}{dx^2} \right)^2 dx \tag{16}$$

where the flexural stiffness and vertical displacement functions are denoted by $EI(x)$ and $w(x)$, respectively.

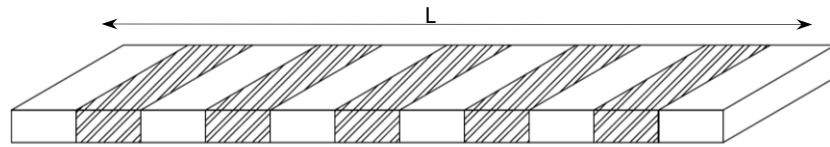


Fig. 1. The finite element model of a beam.

In Eq. (16) and Fig. 1, L is the beam length. Herein, for imposing the boundary conditions, translational and rotational

$$\Pi = \frac{1}{2} \int_0^L EI(x) \left(\frac{d^2 w(x)}{dx^2} \right)^2 dx + \sum_i^{nt} \frac{1}{2} K_i^t w^2(x_i) + \sum_i^{nr} \frac{1}{2} K_i^r w'^2(x_i) \tag{17}$$

In this equation, K_i^t and K_i^r are the stiffness of the i^{th} translational and rotational springs, respectively. Note that the definition of these kinds of springs is available in [24]. In addition, nt and nr denote the number of

springs are deployed. As a consequence, Eq. (16) is rewritten as below [24]:

translational and rotational springs. Moreover, the location of the i^{th} spring is shown by x_i . To estimate the response of the system, the following functions are selected [24]:

$$\Pi = \frac{1}{2} \int_0^L EI(x) \left(\frac{d^2 w(x)}{dx^2} \right)^2 dx + \sum_i^{nt} \frac{1}{2} K_i^t w^2(x_i) + \sum_i^{nr} \frac{1}{2} K_i^r w'^2(x_i) \tag{18}$$

It should be highlighted that the boundary conditions are automatically satisfied by adjusting the stiffness of the aforesaid

springs. These functions are stored in a shape function vector as the coming shape:

$$N_i(x) = \begin{cases} \left(\frac{x}{L} \right)^{i-1} & i = 1, 2, 3 \\ \sin\left(\frac{(i-3)\pi x}{L} \right) + \cos\left(\frac{(i-3)\pi x}{L} \right) & i = 4, 5, \dots, n \end{cases} \tag{19}$$

Note that, number of entries of this vector is n . Consequently, the Ritz solution for the

problem can be expressed as the next form[25]:

$$w(x) = \mathbf{N}(x)\mathbf{B} \tag{20}$$

By applying the principal of virtual displacement, the generalized stiffness and mass matrices can be obtained as below[25]:

$$\mathbf{K} = \int_0^L EI(x) \left(\frac{d^2 \mathbf{N}(x)}{dx^2} \right)^T \left(\frac{d^2 \mathbf{N}(x)}{dx^2} \right) dx \quad (21)$$

$$\mathbf{M} = \int_0^L \rho A(x) \mathbf{N}(x)^T \mathbf{N}(x) dx \quad (22)$$

In these relations, the mass density and the cross-sectional area function of the beam are shown by ρ and $A(x)$, respectively. For the damaged structure, the stiffness matrix has the succeeding appearance[21]:

$$\hat{\mathbf{K}} = \sum_{i=1}^m \left[\int_0^1 (1 - \alpha_D)(\xi) EI_{ei}(\xi) \left(\frac{d^2 \mathbf{N}(\xi)}{d\xi^2} \right)^T \left(\frac{d^2 \mathbf{N}(\xi)}{d\xi^2} \right) |J_i| d\xi \right] \quad (25)$$

$$\hat{\mathbf{M}} = \sum_{i=1}^m \left[\int_0^1 \rho A_{ei}(\xi) \mathbf{N}(\xi)^T \mathbf{N}(\xi) |J_i| d\xi \right]$$

In these relations, $EI_{ei}(\xi)$ and $A_{ei}(\xi)$ are the flexural stiffness and cross-sectional area of the i^{th} element. Moreover, J_i denotes the Jacobian of transformation.

In an undamped and damped structure, natural frequencies and mode shapes can be obtained for damage scenarios with the help of relations (6) and (7), respectively. Note that; the eigenvalues are the natural frequencies of the structure, but the eigenvectors include the coefficients of Eq. (20). By using the next equation, the mode shapes can be achieved[26]:

$$\Psi_i = \mathbf{N}(x)^T \psi_i \quad (27)$$

in which Ψ_i is the eigenvector.

5. Inverse Solution

$$\hat{\mathbf{K}} = \int_0^L (1 - \alpha_D) EI(x) \left(\frac{d^2 \mathbf{N}(x)}{dx^2} \right)^T \left(\frac{d^2 \mathbf{N}(x)}{dx^2} \right) dx \quad (23)$$

Element damage indices can be expressed in natural coordinates as follows:

$$\alpha_D = \alpha_D(\xi) \quad (24)$$

where ξ is the natural coordinate corresponding to each element. Accordingly, the global stiffness and mass matrices can be rewritten as follows, respectively[26]:

Based on the above-mentioned equations, the inverse problem required for estimating the severity and location of damage can be established. In this formulation, the experimental modal data of the damping of structures are needed. It is obvious that the following equation can be written based on orthogonality conditions [22]:

$$\hat{\Psi}^T \hat{\mathbf{K}} \hat{\Psi} = \hat{\Psi}^T \hat{\mathbf{M}} \hat{\Psi} \Omega^2 \quad (28)$$

or,

$$\hat{\Psi}^T \hat{\mathbf{K}} \hat{\Psi} - \hat{\Psi}^T \hat{\mathbf{M}} \hat{\Psi} \Omega^2 = \mathbf{0} \quad (29)$$

where $\hat{\Psi}$ is matrix, which stores the measured mode shapes, and Ω^2 is a diagonal matrix including the square of the measured natural frequencies. Due to applying the Ritz method, the number of rows of these matrices is equal to the number of terms utilized in Ritz solution (n). In other words, their number of rows is equal to the number of unknowns that exist in the response solution. It should be pointed out that the

number of columns of these matrices equals to the number of measured mode shapes. Moreover, it needs to mention that \widehat{K} is replaced by \widehat{K}_d for damped structures. It is worthwhile to highlight that these matrices include the damage indices. Theoretically, the right side of Eq. (29) is a symmetric matrix, having entries equal to zero. However, in practice, it is not true due to the existence of measurement errors.

Accordingly, by extracting the unknown damage indices from the stiffness matrix, the following system of equations can be achieved [21]:

$$\mathbf{A}\boldsymbol{\alpha} = \mathbf{R} \quad (30)$$

In this equality, vector $\boldsymbol{\alpha}$ contains unknown damage indices. Also, \mathbf{A} and \mathbf{R} are the coefficient matrix and residual error vector, respectively. Note that; the number of rows of \mathbf{R} and \mathbf{A} is $s(s+1)/2$. It should be reminded that the number of columns of matrix \mathbf{A} is equal to s . Therefore, this matrix may or may not be square. If number of the rows and columns are not equal, the pseudo-inverse is required for finding $\boldsymbol{\alpha}$ as follows[21]:

$$\boldsymbol{\alpha} = \mathbf{A}^+ \mathbf{R} \quad (31)$$

Where

$$\text{if } \frac{s(s+1)}{2} > s \Rightarrow \mathbf{A}^+ = (\mathbf{A}^T \mathbf{A})^{-1} \mathbf{A}^T \quad (32)$$

$$\text{if } \frac{s(s+1)}{2} < s \Rightarrow \mathbf{A}^+ = (\mathbf{A} \mathbf{A}^T)^{-1} \mathbf{A} \quad (33)$$

In these relations, the pseudo-inverse of the coefficient matrix is denoted by \mathbf{A}^+ .

6. Numerical Examples

In this section, the accuracy and efficiency of the proposed method are evaluated by performing several numerical analyses.

Using a damage scenario in the first step, the mode shapes and natural frequencies of the structure are calculated by using the structural analysis. It should be noted that the Ritz formulation introduced in section 4 is applied for this purpose. In other words, the structural analysis is employed instead of modal tests. By finding the mode shapes and natural frequencies, the authors' damage detection procedure begins. It should be recalled that only a few numbers of mode shapes and natural frequencies are required in the suggested method for estimating the magnitude and location of the damage. It is worthwhile to highlight that a special-purpose program is developed for calculating the mode shapes and natural frequencies based on section 4. Additionally, this program is able to perform damage detection with the help of the proposed method.

6.1. A Two-Span Beam

This section assesses a damaged two-span concrete beam with 0.2m×0.3m cross-section, 0.00045 moment of inertia (I), 25 GPa Young's modulus (E), 2500 kg/m³ density (ρ), and 16 m length (L). For modeling the boundary conditions, the stiffness of the transitional spring (K^t) corresponds to $EI \times 10^5$. It is presumed that the beam includes 16 subdivisions. Note that this beam was previously modeled in [27].

For the problem of damage detection, two patterns are considered by using the two types of stiffness reduction factors applied to some subdivisions. The amounts of stiffness reductions are identical to 5% and 10% for the first damage pattern and 10% and 20% for the second one. Figure 2 illustrates the two damage patterns as well as the

subdivisions with the reduced stiffness. It is clear that the 16 elements of this beam are harmed in these damage patterns. Prior to beginning the damage detection process, the mode shapes, and the first few natural frequencies of these two cases are required.

As previously mentioned, the introduced formulation in section 4 is applied to achieve this goal. It is noticeable that the six natural frequencies and mode shapes of the beam are calculated to use in the two damage scenarios.

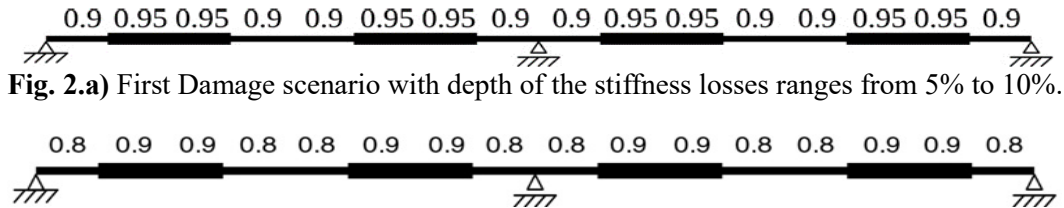


Fig. 2.a) First Damage scenario with depth of the stiffness losses ranges from 5% to 10%.

Fig. 2.b) Second Damage scenario with depth of the stiffness losses ranges from 10% to 20%

Fig. 2. Two-span beam and its damage patterns.

Table 1 lists the six natural frequencies of the damaged and intact conditions estimated from the proposed method and the technique

of Kokot and Zembaty [27]. The information in this table is suitable for the comparison of these methods.

Table 1. The natural frequencies of the intact and damaged two-span beam.

Description of the damaged pattern	f ₁ (Hz)	f ₂ (Hz)	f ₃ (Hz)	f ₄ (Hz)	f ₅ (Hz)	f ₆ (Hz)
Intact [27]	4.48	7.00	17.93	22.70	40.38	47.41
Intact (Present work)	4.48	7.00	17.94	22.75	40.39	47.50
5%&10% damage scenario [27]	4.31	6.71	17.39	21.90	37.19	43.62
5%&10% damage scenario (Present work)	4.31	6.71	17.40	21.94	38.84	45.66
10%&20% damage scenario [27]	4.12	6.40	16.82	21.05	38.83	45.57
10%&20% damage scenario (Present work)	4.13	6.40	16.84	21.10	37.22	43.74

It is obvious that the natural frequencies obtained from the method introduced in section 4 are compatible with those gained by [27]. Therefore, the authors' formulation and their computer program are verified. Obviously, the occurrence of damage reduces the natural frequencies of the beam. This is because of the fact that damage decreases the stiffness of the structure. Now, the damage identification scheme is applied for

estimating the severity and location of the damage. For this purpose, the various modes are applied. The estimated damage indices corresponding to the aforesaid complex damage scenarios are listed in Tables 2 and 3.

It is clear that the proposed damage identification approach is able to successfully find the magnitude and location of damage in this beam by using only a few numbers of mode shapes and natural frequencies.

Table 2. The calculated damage indices corresponding to 5%&10% damage scenario.

Element number	5%&10% damage scenario [27]	5%&10% damage scenario (Present work)		
		By using the first 2 eigenpairs	By using the first 3 eigenpairs	By using the first 4 eigenpairs
1	0.90	0.43	0.94	0.89
2	0.95	0.68	1.16	0.96
3	0.95	1.04	0.84	0.94
4	0.90	1.32	0.77	0.90
5	0.90	1.18	1.09	0.91
6	0.95	0.70	1.12	0.95
7	0.95	0.38	0.74	0.94
8	0.90	0.53	0.61	0.91
9	0.90	0.78	0.88	0.90
10	0.95	0.73	0.95	0.94
11	0.95	0.66	0.73	0.95
12	0.90	0.96	0.80	0.91
13	0.90	1.30	1.15	0.90
14	0.95	1.09	1.11	0.94
15	0.95	0.46	0.58	0.96
16	0.90	0.07	0.21	0.90

Table 3. The calculated damage indices corresponding to 10%&20% damage scenario.

Element number	10%&20% damage scenario [27]	10%&20% damage scenario (Present work)		
		By using the first 2 eigenpairs	By using the first 3 eigenpairs	By using the first 4 eigenpairs
1	0.8	0.39	0.89	0.79
2	0.9	0.62	1.09	0.92
3	0.9	0.95	0.76	0.88
4	0.8	1.21	0.68	0.80
5	0.8	1.09	1.00	0.82
6	0.9	0.65	1.05	0.89
7	0.9	0.35	0.68	0.88
8	0.8	0.48	0.55	0.81
9	0.8	0.70	0.80	0.81
10	0.9	0.67	0.88	0.88
11	0.9	0.62	0.68	0.90
12	0.8	0.89	0.73	0.82
13	0.8	1.19	1.05	0.79
14	0.9	0.99	1.01	0.88
15	0.9	0.41	0.54	0.92
16	0.8	0.07	0.21	0.79

6.2. A Simply-Supported Beam

Here, a simply supported beam mentioned in Gharighoran *et al.* [21] is assessed, which includes ten beam elements. The bending stiffness, cross-sectional area, mass density,

and span length of this beam are assumed to be equal to those of the previous example.

To model the simple supports, translational springs with the stiffness of 10^{+12} kg/m are used. To consider damping for this beam, it is assumed that $\alpha = 4.48$ and $\beta = 4.3 \times 10^{-4}$

A complex damage scenario is considered. This beam and its damage pattern are illustrated in Figure 3. Damage detection is conducted with and without noise.

Now, the first five natural frequencies of the damaged and sound beam are computed. The obtained results are compared with those of [21] in Table 4 for the verification.

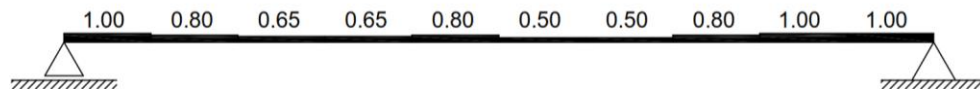


Fig. 3. The simply supported beam with its damage pattern.

Table 4. The natural frequencies of the undamaged and damaged simply supported beam.

Description of the damaged pattern	f_1 (Hz)	f_2 (Hz)	f_3 (Hz)	f_4 (Hz)	f_5 (Hz)
Intact [21]	1.57	6.28	14.15	25.13	39.27
Intact (Present work)	1.58	6.31	14.24	25.31	39.88
Intact (Present work + Damping)	1.58+0.048i	6.31+0.041i	14.24+0.076i	25.31+0.13i	39.89+0.2i
Damaged (Present work + Damping)	1.26+0.056i	5.32+0.038i	12.48+0.067i	21.87+0.11i	34.33+0.17i

It is clear that the proposed approach is successful in finding natural frequencies. Obviously, damage leads to a reduction in stiffness. As a result, the natural frequencies

of the damaged beam are less than the second one. At this stage, the first five mode shapes of the damaged and intact beam are illustrated in Figure 4.

Mode Shapes Damage(DS) and Sound Stage(SS)

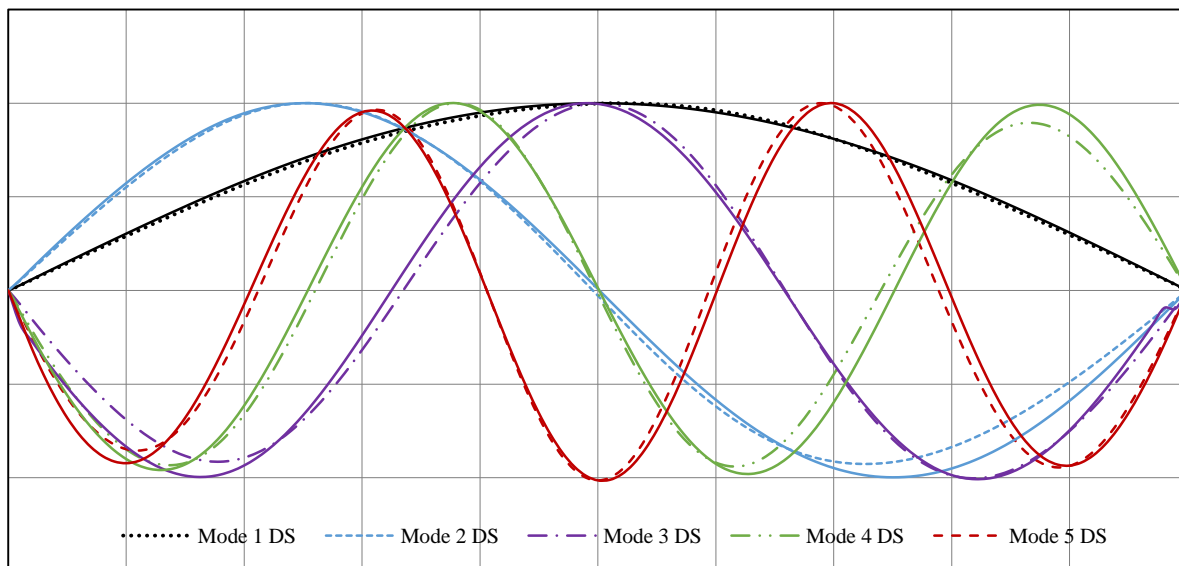


Fig. 4. The damaged and undamaged mode shapes.

Herein, the suggested damage detection method is applied to estimate the damage indices of this structure. For this purpose, only the first five natural frequencies and

mode shapes of the damaged structure are employed. The obtained results are presented in Figure 5.

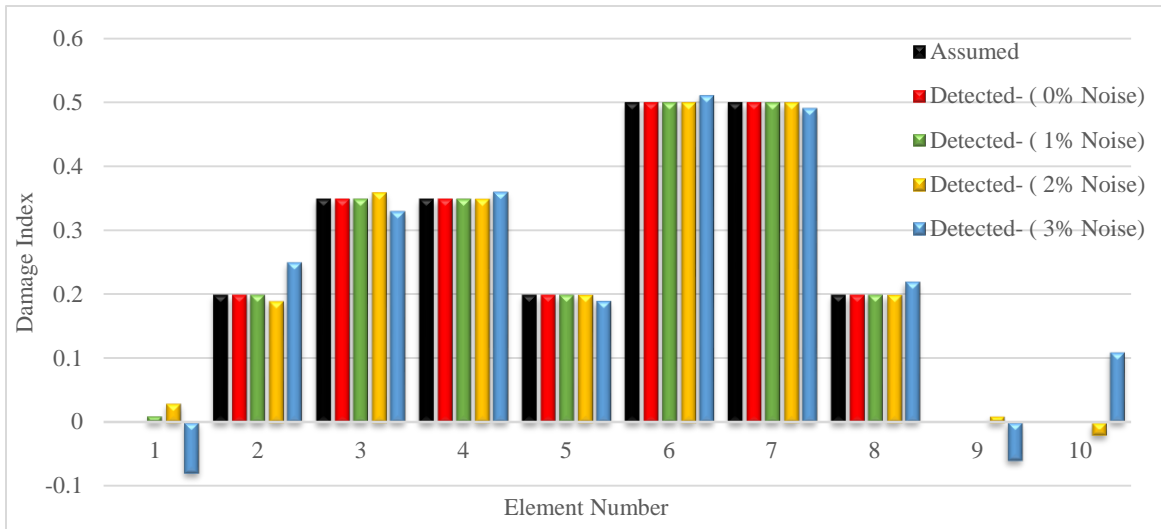


Fig. 5. Detected vs. exact damage indices.

Accordingly, the proposed method is capable of estimating the severity and location of damage in this beam structure with and without noise.

6.3. A Fixed Support Beam

In this subsection, a fixed support beam with $0.3m \times 0.3m$ cross-section is evaluated. It is made of concrete with Young’s modulus 25 Gpa and concrete density $\rho = 2500 \text{ kg/m}^3$. It should be added that the beam length is 10m. To model the fixed supports, translational and rotational springs are used.

Their stiffness equal to 10^{+12} kg/m and 10^{+12} kg.m/m , respectively. To consider damping for this beam, it is assumed that $\alpha = 4.48$ and $\beta = 4.3 \times 10^{-4}$

It is assumed that this beam is divided into 10 elements, and five of them are damaged. Similarly, damage detection is conducted with and without noise.

This beam and its damage pattern are shown in Figure 5.

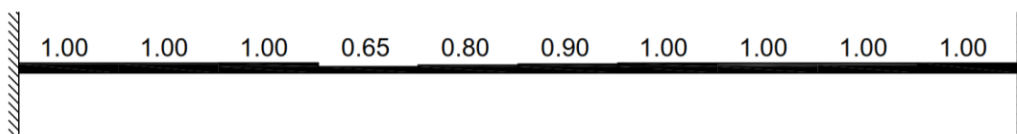


Fig. 6. The fixed support beam with its damage pattern.

Now, its first five natural frequencies are listed in Table 6 for both the damaged and

undamaged cases. For this purpose, the method presented in section 4 is deployed.

Table 6. The natural frequencies of the undamaged and damaged fixed support beam.

Description of the damaged pattern	f_1 (Hz)	f_2 (Hz)	f_3 (Hz)	f_4 (Hz)	f_5 (Hz)
Intact	9.84	27.37	53.95	89.99	135.74
Intact + Damping	9.83+0.055i	27.36+0.14i	53.95+0.27i	89.99+0.45i	135.74+0.68i
Damaged + Damping	9.49+0.054i	26.43+0.13i	52.48+0.26i	85.97+0.43i	128.86+0.64i

Mode Shapes Damage(DS) and Sound Stage(SS)

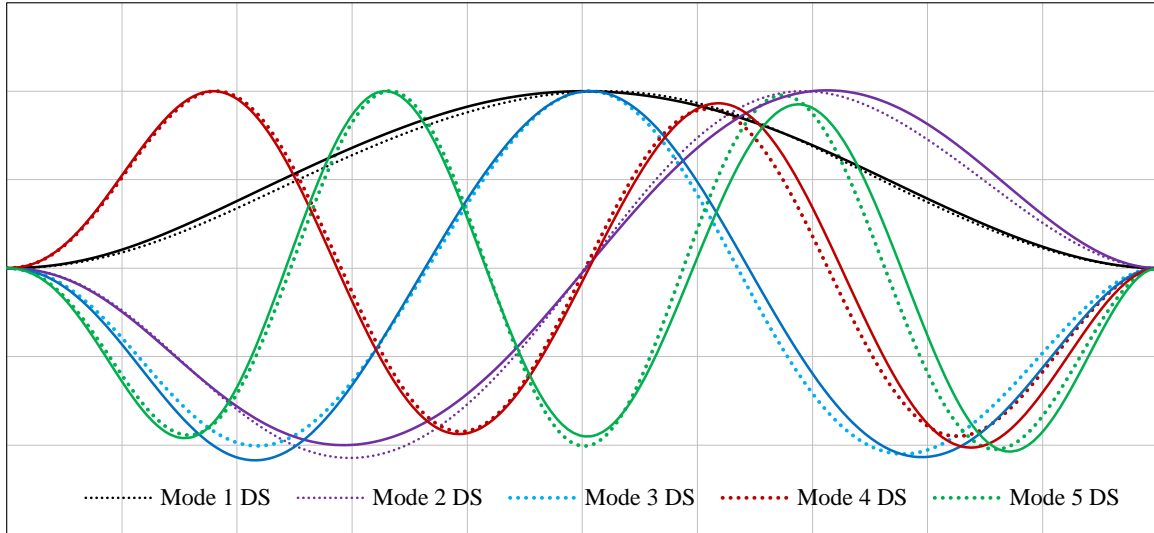


Fig. 7. The damaged and undamaged mode shapes.

Moreover, Figure 7 shows the first five mode shapes of this beam after and prior to damage.

Now, with the help of these five natural frequencies and mode shapes, the proposed damage detection technique calculates the

damage indices. The obtained results are tabulated in Figure 8.

Obviously, the authors' technique is able to find the magnitude and location of damage in this beam with high accuracy.

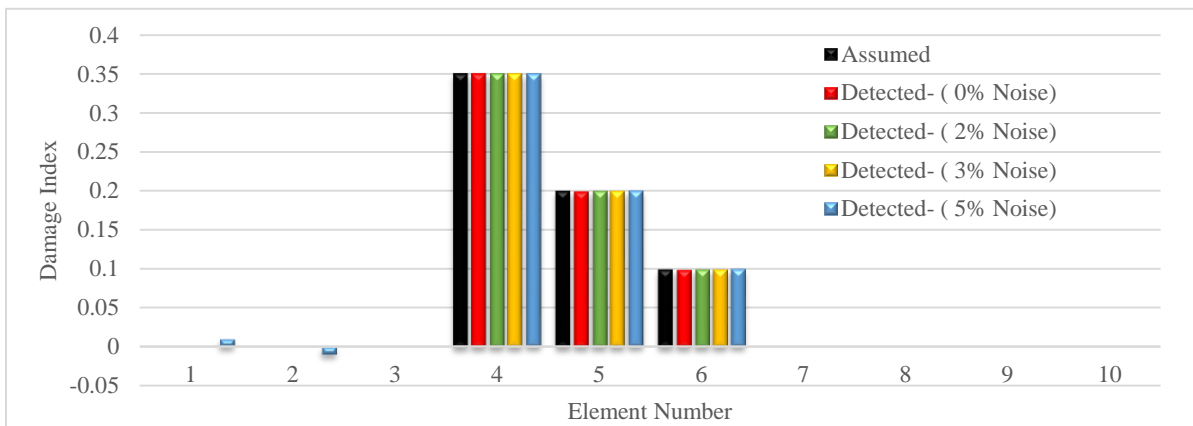


Fig. 8. Detected vs. exact damage indices.

7. Conclusions

Most analytical schemes of damage identification used finite element formulation, and the only limited number of them were developed based on the Rayleigh–Ritz approach. This paper proposed a new damage detection method based on the Rayleigh-Ritz technique. The proposed method is applicable to beam-like structures with any kind of boundary condition, and it only requires a few numbers of natural frequencies and modes shapes of the damaged structure. In this process, lumped rotational and translational springs were utilized for modeling various boundary conditions. Moreover, the proposed method is capable of considering damping. The high robustness and efficiency of the suggested approach were proved by performing different numerical examples. Also, in these examples, the effect of noisy measurement on responses was assessed. The results showed that the proposed approach was successful in damage detection of bridges when the noisy data are available.

REFERENCES

- [1] Larson, A.C. and R. Von Dreele, *Los Alamos National Laboratory Report No.* 1987, LA-UR-86-748.
- [2] Rezaiee-Pajand, M., M.S. Kazemiyan, and A. Aftabi. S, *Static Damage Identification of 3D and 2D Frames*. Mechanics Based Design of Structures and Machines, 2014. 42(1): p. 70-96.
- [3] Haddad, A., D. Rezazadeh Eidgahee, and H. Naderpour, *A probabilistic study on the geometrical design of gravity retaining walls*. World Journal of Engineering, 2017. (14)5: p. 414-422.
- [4] Naderpour, H. and P. Fakharian, *A synthesis of peak picking method and wavelet packet transform for structural modal identification*. KSCE Journal of Civil Engineering, 2016. 20(7): p. 2859-2867.
- [5] Stubbs, N. and J.T. Kim, *Damage localization in structures without baseline modal parameters*. AIAA, 1996. 34: p. 1644-1649.
- [6] Maeck, J., et al., *Damage identification in reinforced concrete structures by dynamic stiffness determination*. Engineering Structures, 2000. 22(10): p. 1339-1349.
- [7] Maeck, J. and G.D. Roeck, *Damage assessment of a gradually damaged rc beam using dynamic system identification, in Kasteelpark Arenberg 40*. Department of Civil Engineering, Structural Mechanics, K.U.Leuven, 2002.
- [8] Kokot, S. and Z. Zembaty, *Damage reconstruction of 3D frames using genetic algorithms with Levenberg–Marquardt local search*. Soil Dynamics and Earthquake Engineering, 2009. 29(2): p. 311-323.
- [9] Yoon, M.-K., et al., *Local Damage Detection with the Global Fitting Method Using Mode Shape Data in Notched Beams*. Journal of Nondestructive Evaluation, 2009. 28(2): p. 63-74.
- [10] Park, J.-H., et al., *Sequential damage detection approaches for beams using time-modal features and artificial neural networks*. Journal of Sound and Vibration, 2009. 323(1): p. 451-474.
- [11] Sung, S.H., K.Y. Koo, and H.J. Jung, *Modal flexibility-based damage detection of cantilever beam-type structures using baseline modification*. Journal of Sound and Vibration, 2014. 333(18): p. 4123-4138.
- [12] Eraky, A., et al., *Damage detection of flexural structural systems using damage index method – Experimental approach*. Alexandria Engineering Journal, 2015. 54(3): p. 497-507.

- [13] Limongelli, M.P., et al., *Damage detection in a post tensioned concrete beam – Experimental investigation*. Engineering Structures, 2016. 128: p. 15-25.
- [14] Deobald, L.R. and R.F. Gibson, *Determination of elastic constants of orthotropic plates by a modal analysis/Rayleigh-Ritz technique*. Journal of Sound and Vibration, 1988. 124(2): p. 269-283.
- [15] Cao, T.T. and D.C. Zimmerman, *Application of Load Dependent Ritz Vectors in Structural Damage Detection, in Conference: 1997 IMAC XV – 15th International Modal Analysis Conference*. 1997. p. 1319-1324.
- [16] Li, Y.Y., et al., *Identification of damage locations for plate-like structures using damage sensitive indices: strain modal approach*. Computers & Structures, 2002. 80(25): p. 1881-1894.
- [17] Sohn, H. and K.H. Law, *Application of load-dependent Ritz vectors to Bayesian probabilistic damage detection*. Probabilistic Engineering Mechanics, 2000. 15(2): p. 139-153.
- [18] Sarker, L., et al., *Damage detection of circular cylindrical shells by Ritz method, in 9th International Conference on Damage Assessment of Structures*. 2011.
- [19] García, P.M., J.V. Araújo dos Santos, and H. Lopes, *A new technique to optimize the use of mode shape derivatives to localize damage in laminated composite plates*. Composite Structures, 2014. 108: p. 548-554.
- [20] Maghsoodi, A., A. Ghadami, and H.R. Mirdamadi, *Multiple-crack damage detection in multi-step beams by a novel local flexibility-based damage index*. Journal of Sound and Vibration, 2013. 332(2): p. 294-305.
- [21] Gharighoran, A., F. Daneshjoo, and N. Khaji, *Use of Ritz method for damage detection of reinforced and post-tensioned concrete beams*. Construction and Building Materials, 2009. 23(6): p. 2167-2176.
- [22] Chopra, A.K., *Dynamics of Structures: Theory and Applications to Earthquake Engineering*. 2007: Pearson/Prentice Hall.
- [23] Doebling, S.W., et al., *Damage identification and health monitoring of structural and mechanical systems from changes in their vibration characteristics: a literature review, in Research report LA-13070-MS, ESA-EA Los Alamos National Laboratory*. 1996: Los Alamos, NM, USA.
- [24] Ilanko, S., L. Monterrubio, and Y. Mochida, *The Rayleigh-Ritz method for structural analysis*. 2015: John Wiley & Sons.
- [25] Alaylioglu, H. and A. Alaylioglu, *Finite element and experimental bases of a practical bridge management and maintenance system*. Computers & Structures, 1999. 73(1-5): p. 281-293.
- [26] Rezaiee-Pajand, M. and M. Moayyedian, *Finite Element Theory*. null. Vol. null. 2004. null.
- [27] Kokot, S. and Z. Zembaty, *Vibration based stiffness reconstruction of beams and frames by observing their rotations under harmonic excitations—numerical analysis*. Engineering Structures, 2009. 31(7): p. 1581-1588.